Synergistic effectiveness of eggshell membranes–supported zinc oxide materials on the removal of organic dyes from wastewater

Qing Lin[a,*], Shuiping Li[b], Qiuying Zhao[c], Wei Wang[a], Xiaojuan Zhang[a], Lingyun Hao[a]

[a]*School of Materials Engineering, Jinling Institute of Technology, Nanjing 211169, China; emails: lnqing@jit.edu.cn (Q. Lin), wangwei@jit.edu.cn (W. Wang), xixi@jit.edu.cn (X. Zhang), hly@jit.edu.cn (L. Hao)*
[b]*College of Materials Science and Engineering, Yancheng Institute of Technology, Yancheng 224051, China; email: lishuiping2002@hotmail.com*
[c]*College of Materials Science and Technology, Nanjing University of Aeronautics and Astronautics, Nanjing 210016, China; email: 57357287@qq.com*

ABSTRACT

The surfaces of eggshell membranes (ESMs) were modified by silane coupling agent (KH550) to form $Si(OH)_4$. ESMs–supported zinc oxide (ZnO) had been successfully fabricated by microwave method. ESMs could keep their original structure and strength after the microwave treatment, and ZnO particles with high oxygen defects were closely supported on the protein fibres of ESMs. After soaking ESMs–supported ZnO materials in organic dyes wastewater for 80 min, they could not only absorb 50% organic dyes by ESMs, but also photodegradate 26% of organic dyes by ZnO. The synergistic effectiveness may significantly improve the treatment efficiencies of ESMs–supported ZnO materials on the organic dyes from the wastewater. ESMs–supported ZnO materials with a synergistic effectiveness may be a potential product for the removal of organic dyes from wastewater in the future.

Keywords: Zinc oxide; Eggshell membranes; Microwave method; Photocatalytic property

1. Introduction

In textile industry, a large amount of water is being used to wash dyed fabrics and remove residual dyes from their surfaces. Textile dyes are difficult to be degraded under natural conditions [1,2], which is owing to the non-oxidizable property by conventional treatments for their complex aromatic structure [3]. Moreover, textile dyes and their breakdown products are carcinogenic or mutagenic to human beings [4,5], primarily due to mutagens and carcinogens such as naphthalene, benzidine, and other aromatic compounds [6,7]. The natural water bodies would be polluted by wastewater containing textile dyes, and unfavourable to use for animals or plants without any treatments [4]. Various techniques have been applied to remove the textile dyes from wastewater. However, conventional biological treatment methods were ineffective for discolouration and degradation of textile dyes. Advanced oxidation processes (AOP) had been developed as a novel treatment method for converting these organic dyes to harmless compounds [8]. Photocatalysis is one kind of the AOP and is carried out under light irradiation with a suitable photocatalytic material. Photocatalytic degradation has been proved to be a successful technique to remove organic dyes from wastewater [9,10]. Zinc oxide (ZnO, 3.37 eV), which exhibits a similar band gap energy to TiO_2 (3.20 eV) [11,12], has been extensively used as the photocatalyst [8]. Moreover, ZnO has physical and chemical stability, low cost, and high oxidative capacity. ZnO is a *n*-type semiconductor, and the electron–hole pairs are generated by means of bandgap radiation [2,3]. The photoelectrons and holes are beneficial to photocatalytic reactions.

ZnO could decompose organic dyes to H_2O and CO_2 by using solar light without any extra energy [13]. Former researches also indicated that ZnO particles with high surface

* Corresponding author.

areas showed an excellent photocatalytic activity on the degradation of organic dyes under the solar light irradiation [8]. However, there is a key technical barrier for the application of ZnO particles as a photocatalyst. If ZnO particles do not have a suitable supporter, they would be hard to be recycled and even lead to a secondary pollution [14].

As it is well known, eggshell membranes (ESMs) show an excellent adsorption property, and are environmentally friendly and non-toxic [15]. However, ESMs have a low utilization rate. ESMs would have a potential value in the removal of organic dyes from wastewater, when they were used as the supporter for ZnO particles. The adsorption and photocatalysis methods could be combined to remove textile dyes from wastewater [1], when they were used as the supporter for ZnO particles. Although there are many methods that had been applied to fabricate ESMs–supported ZnO materials (ZnO-ESMs) [16], to avoid destroying the original structure and strength of ESMs, microwave method was employed to synthesis ZnO-ESMs [17]. The synergistic effectiveness of ZnO-ESMs on the removal of organic dyes from wastewater were evaluated in this study.

2. Experimental procedure

2.1. Materials

Zinc acetate ($Zn(Ac)_2$), sodium hydroxide (NaOH), and 3-aminopropyltriethoxy silane coupling agent (KH550) were used as raw materials. $Zn(Ac)_2$, NaOH, and KH550 were purchased from Chinese Medicine Group Chemical Reagent Co., Ltd., Shanghai. ESMs were peeled from the fresh eggs and washed with the deionized water. Then, ESMs were soaked in the KH550 solution (4 wt%) for 24 h, and these soaked ESMs were defined as Si-ESMs. Subsequently, ESMs and Si-ESMs were immersed into 0.01 mol·L^{-1} $Zn(AC)_2$ solutions for 2 h with a surface area to volume ratio at 0.4 cm^{-1}. 0.1 mol·L^{-1} of NaOH solutions were dropped into the above solutions with a $n(OH^-)/n(Zn^{2+})$ ratio at 2.0, and the mixtures were continuously stirred for 30 min. Afterwards, the mixtures were further heated in a microwave oven (G80F, Gelanz, China) for 5 min under an ordinary pressure. The reaction temperature was always lower than 100°C. The obtained samples were named as ZnO-ESMs and Si-ESMs–supported ZnO materials (ZnO-Si-ESMs). Finally, ZnO-ESMs and ZnO-Si-ESMs were washed with deionized water and dried at 60°C for further characterizations.

2.2. Characterization

The crystal phases of ZnO on the surfaces of ZnO-ESMs and ZnO-Si-ESMs were determined by X-ray diffractometer (XRD, D/MAX-2500/PC; Rigaku, Tokyo, Japan) at a scanning speed of 10° min^{-1} with CuK$_\alpha$ radiation. The functional groups in ESMs and Si-ESMs were analyzed using attenuated total reflection-Fourier-transform infrared spectrometer (ATR-FTIR, Nicolet iS10, Thermo Nicolet, United States) with a resolution of 2 cm^{-1} and a scan number of 32. The surface morphologies of ESMs, ZnO-ESMs, and ZnO-Si-ESMs were characterized using a field emission scanning electron microscopy (SEM, Hitachi, SU8010, Japan) with a 3.0 kV operating voltage. To further characterize the optical properties of ZnO particles,

the photoluminescence (PL) spectra were measured with an excitation wavelength of 350 nm using alpha (NSOM, WITec, Germany) near-field scanning optical microscopy system at the room temperature. The contact angle analyzer (JY-82, Chengde Experimental Machine Plant, China) was used to evaluate the hydrophilicity of ESMs and Si-ESMs. Approximately, 5 μL distilled water was dropped on the surfaces of ESMs and Si-ESMs before measuring. All data were presented by the mean values of six independent measurements.

2.3. Photocatalytic experiments

Rhodamine B (RB) is a kind of reactive dyes and is mostly used for the dyeing of natural fibres such as wool, cotton, and silk. In this study, RB aqueous solution was used to simulate the organic dyes wastewater. The RB adsorption of ESMs was determined by soaking ESMs in a 20-mg·L^{-1} RB solution with a volume of RB solution to the surfaces of ESMs ratio at 5 mL·cm^{-2}. The mixture was stirred at room temperature, and the remaining RB concentration in solution was determined by the UV spectrophotometer (TU-1901, China) at the given time. The control sample of photocatalytic experiments was determined under the UV irradiation (60 W), and the control sample was pure RB solution without ESMs, ZnO-ESMs, or ZnO-Si-ESMs. To evaluate the photocatalytic properties of ZnO-ESMs and ZnO-Si-ESMs, 20 mg·L^{-1} RB solutions were photodegraded under UV irradiation (60 W) with a magnetic stirrer at room temperature [18]. The ratios of the volumes of RB solution to the surfaces of ZnO-ESMs (or ZnO-Si-ESMs) were kept at 5 mL·cm^{-2}. The remaining RB concentration in solution was determined by the UV spectrophotometer at the giving time. Finally, the degradation rate curves of ZnO-ESMs and ZnO-Si-ESMs were drawn. The removal percentage of RB was calculated from the following equation:

$$\eta(\%) = \frac{C_0 - C_t}{C_0} \times 100 \tag{1}$$

where C_0 is the initial RB concentration, and C_t is the final concentration after the photocatalytic treatment.

3. Results and discussion

ATR-FTIR spectra of ESMs and Si-ESMs are shown in Fig. 1. The major bands for ESMs could be assigned as follows: 1,724 cm^{-1} (C=O stretching mode assigned to the amide I vibration) [15]; 1,599 and 1,227 cm^{-1} (C–N stretching/N–H bending modes assigned to amide II and amide III vibrations, respectively) [19]; and 680 cm^{-1} (C–S stretching vibrations) [20]. Compared with ESMs, Si-ESMs showed a new weak vibration peak at 1,030 cm^{-1}, which was attributed to Si-O-Si stretching vibration [21]. The peak at 1,450 cm^{-1} was ascribed to the stretching vibration band of C–N in KH550 [22]. Moreover, two N–H stretching vibration peaks in KH550 were observed at 1,528 and 751 cm^{-1} [22], receptivity. It indicated that the surfaces of Si-ESMs had been successfully modified by KH550.

The hydrophilicities of ESMs and Si-ESMs were examined by water contact angle measurement. The outside surfaces of ESMs were a meshwork composed of interwoven

Fig. 1. ATR-FTIR spectra of ESMs and Si-ESMs.

Fig. 2. Contact angle images of wet (a) ESMs and (b) Si-ESMs.

Fig. 3. XRD patterns of the surfaces of ZnO-ESMs and ZnO-Si-ESMs.
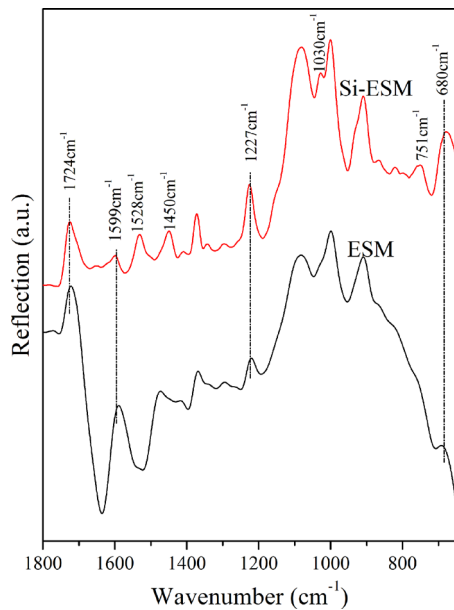
Fig. 4. Photoluminescence (PL) spectra of ZnO-ESMs and ZnO-Si-ESMs.

and coalescing micron fibres, and a large amount of hydrophilic groups existed [15]. This might endow the hydrophilicity of ESMs. As seen from Fig. 2, Si-ESM (12.4° ± 2.0) had a lower contact angle than ESMs (38.5° ± 1.6). This difference indicated that Si-ESMs were more hydrophilic than ESMs. Si-ESMs modified by KH550 showed a better hydrophilicity than ESMs, and Si-ESMs surfaces would be more suitable to support ZnO particles. Because KH550 was hydrolyzed in this condition, Si-O-R groups in KH550 were mostly converted into Si-OH groups on Si-ESMs surfaces.

XRD patterns of the surfaces of ZnO-ESMs and ZnO-Si-ESMs are shown in Fig. 3. All diffraction peaks matched the hexagonal wurtzite crystal structure of ZnO [11]. It indicated that no impurity appeared in the three peaks of 31.65°, 34.44°, and 36.24°. The diffraction peaks of ZnO on the surfaces of ZnO-Si-ESMs were broadened, and grain sizes of ZnO on ZnO-Si-ESMs were remarkably decreased by using KH550 [23]. It indicated the ZnO particles had been strongly supported on ESMs surfaces by hydrothermal treatment in the microwave oven under an ordinary pressure. According to the Scherrer formula ($D = K\lambda/B \cos\theta$) [23], the grain sizes of ZnO particles on ZnO-ESMs and ZnO-Si-ESMs were about 90 and 18 nm, respectively.

The PL spectra of ZnO-ESMs and ZnO-Si-ESMs are shown in Fig. 4. All samples revealed a weak UV emission centred at 391 nm and a strong visible emission in the range of 425–600 nm [24]. According to the studies on PL spectra of ZnO, the UV emission can be due to the near band-edge transition, while the visible emission can be due to the transitions in the intrinsic or extrinsic defect states [25]. This green visible emission was often attributed to oxygen vacancies or zinc interstitials [26]. ZnO particles on ESMs with surface oxygen defects, which served as adsorption active sites, can be excited by visible and UV light due to the narrow energy band gap. The concentration of oxygen defects becomes higher as the PL peak of green visible emission was stronger, which would be beneficial to photocatalysis [27].
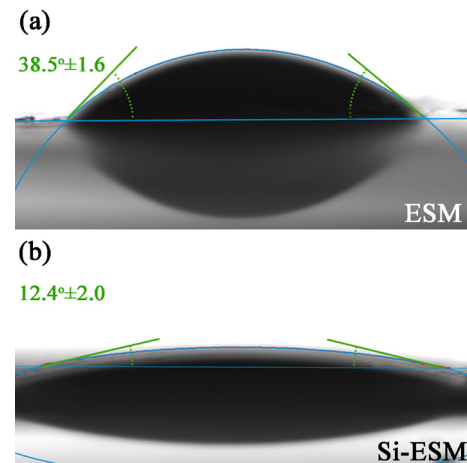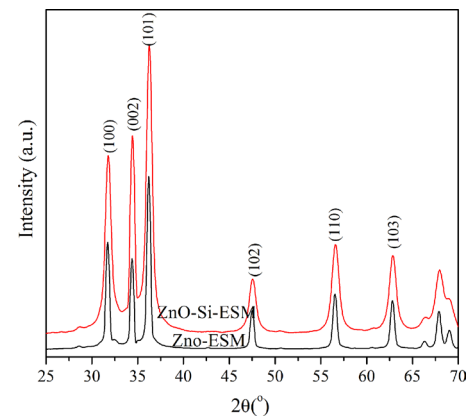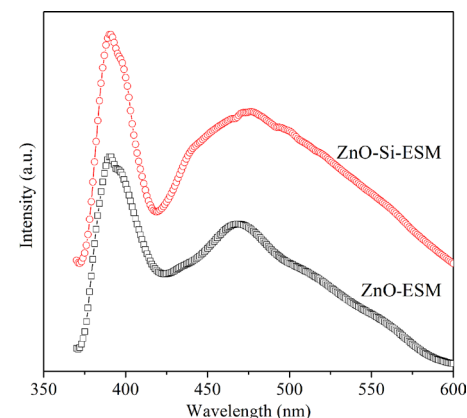
SEM micrographs of ESM, ZnO-ESMs, and ZnO-Si-ESMs are shown in Fig. 5. Protein fibres were intricate and fascinating(Fig. 5(a)), and ESMs showed an intricate lattice network [28]. ZnO particles on the surfaces of ZnO-ESMs were homogeneous and distributed in the pores or spaces between fibres (Figs. 5(c) and (d)). ESMs were not damaged when they
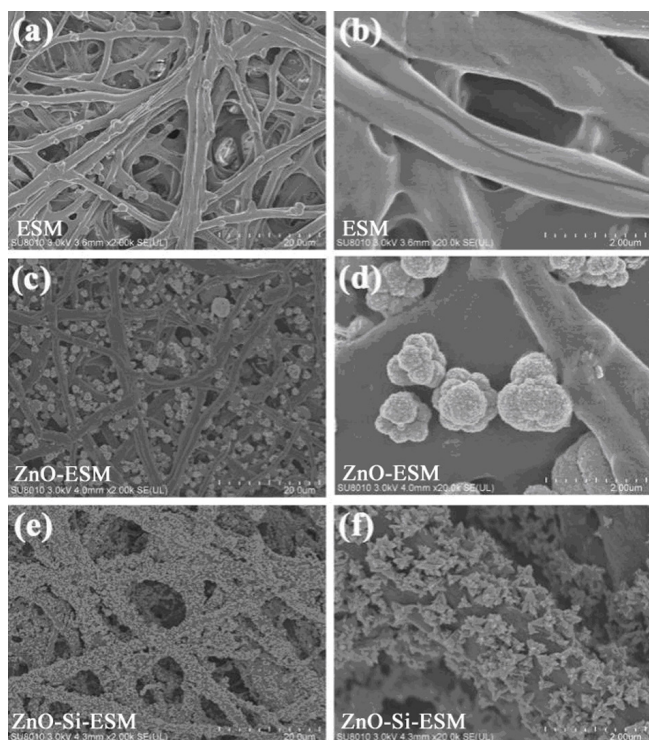
Fig. 5. SEM micrographs of ((a) and (b)) ESMs, ((c) and (d)) ZnO-ESMs, and ((e) and (f)) ZnO-Si-ESMs.

Fig. 6. (a) The adsorption curve of ESMs in RB solution and (b) the photocatalytic degradation profiles of the control, ZnO-ESMs, and ZnO-Si-ESMs for RB under UV irradiation.

were heated in a microwave oven under an ordinary pressure. ZnO particles on the surfaces of ZnO-Si-ESMs were no longer similar to the spherical particles than those on the surface of ZnO-ESMs. ZnO particles were more tightly supported on ZnO-Si-ESMs surfaces (Figs. 5(e) and (f)). Si-OH on Si-ESMs modified by KH550 may be functioned as the deposited sites for the formation of ZnO particles [21]. SEM micrographs indicated that KH550 had improved the dispersion and adhesion of ZnO on ESMs.

The adsorption curve of ESMs in RB solution is shown in Fig. 6(a). ESMs had a strong adsorption of RB at a low concentration. ESMs had absorbed about 50% RB after soaking them in RB solutions for 80 min. However, the adsorption presents of RB could not be increased with the increased soaking time. It soundly illustrated that ESMs could absorb organic dyes in wastewater. To evaluate the photocatalytic properties of ZnO-ESMs and ZnO-Si-ESMs, the photocatalytic decomposition of RB was performed as a test reaction according to previous literature [18]. As depicted in Fig. 6(b), RB concentrations in the solutions soaking with ZnO-ESMs and ZnO-Si-ESMs were rapidly decreased under the irradiation of UV light. Moreover, RB concentrations in the solutions soaking with ZnO-ESMs and ZnO-Si-ESMs (Fig. 6(a)) were obviously lower than those in the solutions soaking with ESMs at the given times (Fig. 6(b)). These may attribute to the adsorption performance of ESMs and the photocatalytic property of ZnO [29]. ZnO-Si-ESMs exhibited a better photocatalytic property than ZnO-ESMs, because more ZnO particles were loaded on ZnO-Si-ESMs (Fig. 5). Under the UV irradiation, RB was firstly de-ethylated in a stepwise manner [30]. The dispersion colour of RB solution was changed from an initial red to a light green-yellow. The de-ethylated RB was identified as the intermediate, and the completely
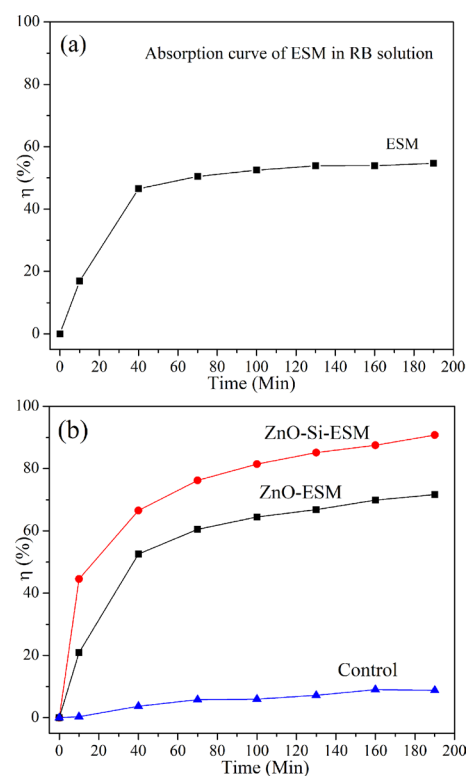
de-ethylated RB has a major absorption band at 498 nm [31]. De-ethylated RB was further degraded through the destruction of the conjugated structure [30,32]. The dispersion colour of RB solution would disappear because the chromophoric structure in RB was destroyed. By subtracting the adsorption content of ESMs (50 %), it was calculated that ZnO on ZnO-Si-ESMs might photocatalytic degrade about 26% RB in the solution under the UV irradiation for 80 min (Fig. 6).

SEM micrographs of ESMs and ZnO-Si-ESMs after adsorption of RB are shown in Fig. 7. SEM micrograph of ESMs also showed an intricate lattice network after adsorption of RB [28]. However, the diameters of protein fibres (Fig. 7(a)) were increased as comparing with those of the original protein fibres (Fig. 5(a)). Protein fibres were completely coated by RB, original protein fibres could be found (Fig. 7(b)) when the RB coating was broken (shown in white arrow). ZnO particles on ZnO-Si-ESMs could not been seen clearly. The surfaces of ZnO-Si-ESMs were completely coated by RB as the result of the adsorption effect of ESMs on RB. RB showed a leaf-like structure on ZnO-Si-ESMs, which was different from those on ESMs. This may be attributed to the difference of their original surface micrographs (Fig. 5). The results further indicated that ESMs had a strong adsorption effect on RB.

ATR-FTIR spectrum of ZnO-Si-ESMs after adsorption of RB is shown in Fig. 8. Compared with ZnO-Si-ESMs (Fig. 1(c)), two new peaks at 798 and 1,257 cm⁻¹ appeared after the adsorption of RB (Fig. 8), respectively. The 798 cm⁻¹ peak can be assigned to the C–H out of plane bending in RB [33,34]. The peak at 1,257 cm⁻¹ was assigned to the aromatic skeletal C–O–C stretch in RB [33].
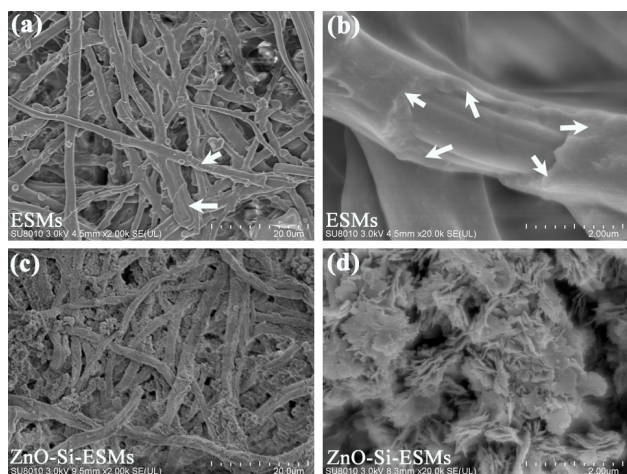
Fig. 7. SEM micrographs of ((a) and (b)) ESMs and ((c) and (d)) ZnO-Si-ESMs after adsorption of Rhodamine B (RB).

Fig. 8. ATR-FTIR spectrum of ZnO-Si-ESMs after adsorption of Rhodamine B (RB).

Fig. 9. The schematic mechanism of eggshell membranes (ESMs)-supported ZnO materials ((a) ESMs, (b) ESM fibers, (c) ESM fibers modified with the silane coupling agent and (d) ESM supported ZnO materials).

To solve the recycling of ZnO particles in the applications, traditional hydrothermal method had been adopted to support ZnO on the different carriers, such as zeolite [35], Si substrate [36], sapphire [37], and Al substrate [38]. As it is well known that ESMs would degrade under high temperature or pressure, the traditional hydrothermal method was not suitable for ESMs. Microwave method had been successfully applied to prepare ZnO-ESMs without any damage to ESMs. Moreover, HK550 played a key role on the supporting of ZnO on ESMs surfaces. Adsorption is one of the best solutions for the removal of dyes from the wastewater due to its cost-effective nature [4,7]. The adsorption of ESMs has been effectively applied, and the organic dye treatment efficiencies of ZnO-ESMs had been significantly improved. ZnO-ESMs have a synergistic effect on the removal of organic dyes from wastewater. The advantages of ZnO-ESMs were that they could be easily separated from the treated wastewater, and the dangerous effects of contamination due to ZnO particles in wastewater could be avoided. The combined adsorption–photocatalysis of dyes was more efficient [2].

Then, a possible mechanism for the formation of ZnO-ESMs was proposed as shown in Fig. 9. Although ESMs are an abundant industrial and household waste, ESMs are environmentally friendly and non-toxic. ESMs are composed of highly interwoven protein fibres (Fig. 9(b)). ESMs have a crucial role in the mineralization of eggshell, which is mainly composed of calcium carbonate. In contrast, ZnO is not easily supported on the ESMs surfaces. KH550 was used as a coupling agent to modify the surface chemical properties of ESMs, because KH550 could absorb on ESMs by the formation of hydrogen bond, and the surface of ESMs would mainly consists of $Si(OH)_4$ after the hydrolysis of KH550 (Fig. 9(c)). The presence of $Si(OH)_4$ was relatively dependent on the peak at 1,030 cm^{-1} in the FTIR spectra (Fig. 1). $Si(OH)_4$ provided the negatively charged sites for migration of Zn^{2+} and OH^- to the surfaces of ESMs, followed by the deposition and growth of $Zn(OH)_2$. Finally, $Zn(OH)_2$ decomposed to ZnO after microwave treatment. Microwave method provided a rapid and homogeneous heating for the decomposition of $Zn(OH)_2$ to ZnO (Fig. 9(d)) under the ordinary temperature and pressure. So ESMs were protected without any damages (Fig. 5). ESMs could be considered as an efficient adsorbent due to their high surface areas, amendable shape, and biocompatible nature. ESMs possess excellent adsorption abilities on organic dyes (such as RB in Fig. 6(a)). It was believed that the ESMs could substitute the conventional carriers and adsorbents. The adsorption performances of ESMs and the photocatalysis of ZnO have been effectively combined and applied; the adsorption and photocatalysis phenomena are working contemporary to each other at the same time [2]. ZnO-ESMs could not only absorb organic dyes by ESMs, but also photodegradate organic dyes by ZnO. ZnO-ESMs had a synergistic effect on the removal of organic dyes from wastewater. Moreover, ESMs had been successfully used as a suitable supporter for ZnO particles. ZnO-ESMs could be easily
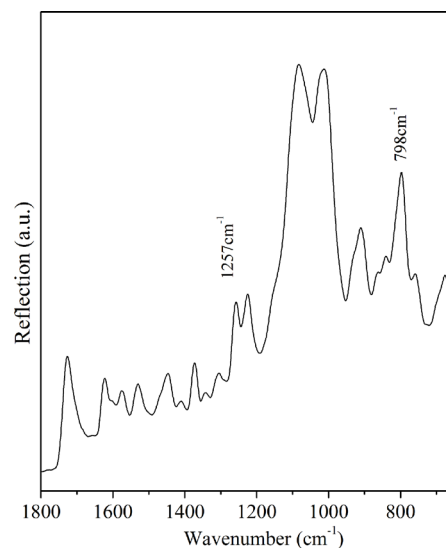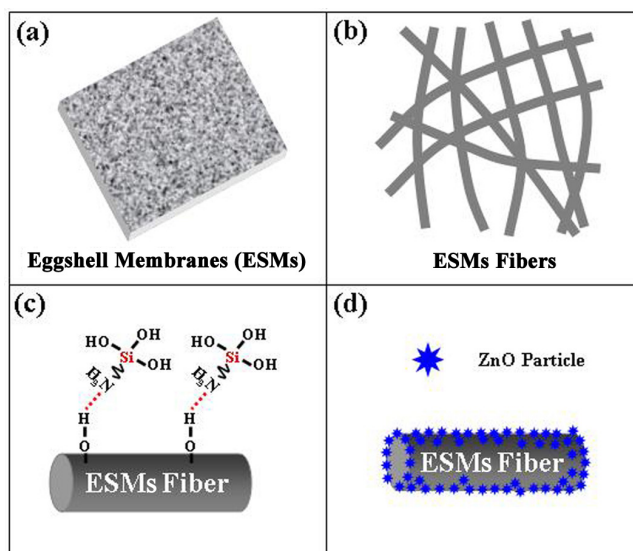
recycled from the wastewater by filter and then reused. As described above, ZnO-ESMs may be developed as a potential product for the wastewater treatment in the future.

4. Conclusion

The surface of ESMs was modified by KH550 to support ZnO particles. ZnO-ESMs had been successfully fabricated by microwave method. ESMs could keep their original structure, and ZnO particles with high oxygen defects were closely supported on the protein fibre surfaces of ESMs. ZnO-ESMs could not only absorb organic dyes by ESMs, but also photo-degradate organic dyes by ZnO. The adsorption performance of ESM and the photocatalysis of ZnO had been effectively applied, and the organic dye treatment efficiencies of ZnO-ESMs had been significantly improved. ZnO-ESMs presented a synergistic effect on the removal of organic dyes from wastewater. The advantages of ZnO-ESMs were that they could be easily separated from the treated wastewater, and the dangerous effects of contamination due to ZnO particles in wastewater could be avoided. ZnO-ESMs with the excellent properties may be developed as a potential product for the treatment of organic dyes in the wastewater in the future.

References

[1] D. Pathania, D. Gupta, AaH. Al-Muhtaseb, G. Sharma, A. Kumar, M. Naushad, T. Ahamad, S.M. Alshehri, Photocatalytic degradation of highly toxic dyes using chitosan-g-poly(acrylamide)/ZnS in presence of solar irradiation, J. Photochem. Photobiol., A, 329 (2016) 61–68.
[2] D. Pathania, G. Sharma, A. Kumar, M. Naushad, S. Kalia, A. Sharma, Z.A. Al-Othman, Combined sorptional–photocatalytic remediation of dyes by polyaniline Zr(IV) selenotungstophosphate nanocomposite, Toxicol. Environ. Chem., 97 (2015) 526–37.
[3] A.B. Albadarin, M. Charara, B.J. Abu Tarboush, M.N.M. Ahmad, T.A. Kurniawan, M. Naushad, G.M. Walker, C. Mangwandi, Mechanism analysis of tartrazine biosorption onto masau stones; a low cost by-product from semi-arid regions. J. Mol. Liq., 242 (2017) 478–483.
[4] M. Naushad, Z. Abdullah Alothman, M. Rabiul Awual, S.M. Aladul, T. Ahamad, Adsorption of rose Bengal dye from aqueous solution by amberlite Ira-938 resin: kinetics, isotherms, and thermodynamic studies, Desal. Wat. Treat., 57 (2016) 13527–13533.
[5] D. Pathania, R. Katwal, G. Sharma, M. Naushad, M.R. Khan, A.H. Al-Muhtaseb, Novel guar gum/Al$_2$O$_3$ nanocomposite as an effective photocatalyst for the degradation of malachite green dye, Int. J. Biol. Macromol., 87 (2016) 366–374.
[6] E. Daneshvar, A. Vazirzadeh, A. Niazi, M. Kousha, M. Naushad, A. Bhatnagar, Desorption of methylene blue dye from brown macroalga: effects of operating parameters, isotherm study and kinetic modeling, J. Cleaner Prod., 152 (2017) 443–453.
[7] G. Sharma, M. Naushad, A. Kumar, S. Rana, S. Sharma, A. Bhatnagar, F.J. Stadlar, A.A. Ghfar, M.R. Khan, Efficient removal of coomassie brilliant blue R-250 dye using starch/poly(alginic acid-cl-acrylamide) nanohydrogel, Process Saf. Environ. Prot., 109 (2017) 301–310.

[8] Y. Abdollahi, A. Zakaria, N.A. Sairi, Degradation of high level m-cresol by zinc oxide as photocatalyst, Clean Soil Air Water, 42 (2014) 1292–1297.
[9] A. Yousef, N. A.M. Barakat, T. Amna, A.R. Unnithan, S.S. Al-Deyab, H.Y. Kim, Influence of CdO-doping on the photoluminescence properties of ZnO nanofibers: effective visible light photocatalyst for waste water treatment, J. Lumin., 132 (2012) 1668–1677.
[10] S.M. Lam, J.C. Sin, A.Z. Abdullah, A.R. Mohamed, Degradation of wastewaters containing organic dyes photocatalysed by zinc oxide: a review, Desal. Wat. Treat., 41 (2012) 131–169.
[11] S. Chakrabarti, B.K. Dutta, Photocatalytic degradation of model textile dyes in wastewater using ZnO as semiconductor catalyst, J. Hazard. Mater., 112 (2004) 269–278.
[12] S.D. Marathe, V.S. Shrivastava, Removal of hazardous Ponceau S dye from industrial wastewater using nano-sized ZnO, Desal. Wat. Treat., 54 (2015) 2036–2040.
[13] M. Kahouli, A. Barhoumi, A. Bouzid, A. Al-Hajry, S. Guermaizi, Structural and optical properties of ZnO nanoparticles prepared by direct precipitation method, Superlattices Microstruct., 85 (2015) 7–23.
[14] Z.G. Doğaroğlu, N. Köleli, TiO$_2$ and ZnO nanoparticles toxicity in barley (*Hordeum vulgare* L.), Clean Soil Air Water, 45 (2017) 1700096.
[15] S. Park, K.S. Choi, D. Lee, D. Kim, K.T. Lim, K.H. Lee, H. Seonwoo, J. Kim, Eggshell membrane: review and impact on engineering, Biosyst. Eng., 151 (2016) 446–463.
[16] Y. Wang, X. Li, N. Wang, X. Quan, Y. Chen, Controllable synthesis of ZnO nanoflowers and their morphology-dependent photocatalytic activities, Sep. Purif. Technol., 62 (2008) 727–732.
[17] H. Liu, Z.F. Zhu, D. Yang, H.J. Sun, Microwave assisted hydrothermal synthesis of hierarchical structured ZnO nanorods, Mater. Technol., 26 (2011) 62–66.
[18] N. Daneshvar, S. Aber, M.S. Seyed Dorraji, A.R. Khataee, M.H. Rasoulifard, Photocatalytic degradation of the insecticide diazinon in the presence of prepared nanocrystalline ZnO powders under irradiation of UV-C light, Sep. Purif. Technol., 58 (2007) 91–98.
[19] Y. Li, A. Wang, Y. Bai, S. Wang, Evaluation of a mixed anionic-nonionic surfactant modified eggshell membrane as an advantageous adsorbent for the solid-phase extraction of Sudan I-IV as model analytes, J. Sep. Sci., 40 (2017) 2591–2602.
[20] J. Li, D.H.L. Ng, R. Ma, Z. Min, S. Peng, Eggshell membrane-derived MgFe$_2$O$_4$ for pharmaceutical antibiotics removal and recovery from water, Chem. Eng. Res. Des., 126 (2017) 123–133.
[21] X. Shang, Y. Zhu, Z. Li, Surface modification of silicon carbide with silane coupling agent and hexadecyl iodiele, Appl. Surf. Sci., 394 (2017) 169–77.
[22] B. Wei, Q. Chang, C. Bao, L. Dai, G. Zhang, F. Wu, Surface modification of filter medium particles with silane coupling agent KH550, Colloids Surf., A, 434 (2013) 276–280.
[23] A.L. Patterson, The Scherrer formula for X-ray particle size determination, Phys. Rev., 56 (1939) 978–982.
[24] P. Zhang, B. Li, Z. Zhao, C. Yu, C. Hu, S. Wu, J. Qiu, Furfural-induced hydrothermal synthesis of ZnO@C gemel hexagonal microrods with enhanced photocatalytic activity and stability, ACS Appl. Mater. Interfaces, 6 (2014) 8560–8566.
[25] F. Xu, Y. Lu, Y. Xie, Y. Liu, Synthesis and photoluminescence of assembly-controlled ZnO architectures by aqueous chemical growth, J. Phys. Chem. C, 113 (2009) 1052–1059.
[26] M.M. Ovhal, A. Santhosh Kumar, P. Khullar, M. Kumar, A.C. Abhyankar, Photoluminescence quenching and enhanced spin relaxation in Fe doped ZnO nanoparticles, Mater. Chem. Phys., 195 (2017) 58–66.
[27] X. Bai, L. Wang, R. Zong, Y. Lv, Y. Sun, Y. Zhu, Performance enhancement of ZnO photocatalyst via synergic effect of surface oxygen defect and graphene hybridization, Langmuir, 29 (2013) 3097–3105.
[28] K. Suyama, Y. Fukazawa, Y. Umetsu, A new biomaterial, hen egg shell membrane, to eliminate heavy metal ion from their dilute waste solution, Appl. Biochem. Biotechnol., 45 (1994) 871–879.

[29] T. Xu, L. Zhang, H. Cheng, Y. Zhu, Significantly enhanced photocatalytic performance of ZnO via graphene hybridization and the mechanism study, Appl. Catal., B, 101 (2011) 382–387.

[30] H. Fu, C. Pan, W. Yao, Y. Zhu, Visible-light-induced degradation of rhodamine B by nanosized Bi_2WO_6, J. Phys. Chem. B, 109 (2005) 22432.

[31] F. Chen, J. Zhao, H. Hidaka, Highly selective deethylation of rhodamine B: adsorption and photooxidation pathways of the dye on the composite photocatalyst, Int. J. Photoenergy, 5 (2003) 209–217.

[32] G. Colon, S. Murcia Lopez, M.C. Hidalgo, J.A. Navio, Sunlight highly photoactive Bi_2WO_6-TiO_2 heterostructures for rhodamine B degradation, Chem. Commun., 46 (2010) 4809–4811.

[33] L. Chen, Z. Fang, Modifying luminescent metal-organic frameworks with rhodamine dye: aiming at the optical sensing of anthrax biomarker dipicolinic acid, Inorg. Chim. Acta, 477 (2018) 51–58.

[34] Z. Wang, D. Shen, F. Shen, C. Wu, S. Gu,, Kinetics, equilibrium and thermodynamics studies on biosorption of Rhodamine B from aqueous solution by earthworm manure derived biochar, Int. Biodeterior Biodegrad., 120 (2017) 104–114.

[35] L. Zhao, Z. C. Liu, Z. F. Liu, Synthetic zeolite supported ZnO nanoparticle materials for photocatalytic applications, Mater. Technol., 30 (2015) 60–64.

[36] M. Fang, Z.W. Liu, Controllable size and photoluminescence of ZnO nanorod arrays on Si substrate prepared by microwave-assisted hydrothermal method, Ceram. Int., 43 (2017) 6955–6962.

[37] H. Wu, Z. Hu, B. Li, H. Wang, Y. Peng, D. Zhou, X. Zhang, High-quality ZnO thin film grown on sapphire by hydrothermal method, Mater. Lett., 161(2015) 565–567.

[38] W. Li, S. Gao, L. Li, S. Jiao, Q. Yu, H. Li, J. Wang, Q. Yu, Y. Zhang, D. Wang, A facile solution synthesis of ZnO nanoplates on Al substrate at room temperature, Mater. Lett., 185 (2016) 161–164.